CRYSTAL GROWTH & DESIGN

Article

Cite This: *Cryst. Growth Des.* 2019, 19, 6184−6191

pubs.acs.org/crystal

Morphology, Molecular Orientation, and Solid-State Characterization of 2,3-Dihydrothieno[3,4-*b*][1,4]dioxine-2-carboxylic Acid (EDOTacid)

Vivek Subramanian,[†] Casey A. Rowland,[‡] Glenn P. A. Yap,[‡] and David C. Martin*[,†,§]

[†]Department of Materials Science and Engineering, [‡]Department of Chemistry and Biochemistry, and [§]Department of Biomedical Engineering, The University of Delaware, Newark, Delaware 19716, United States

Supporting Information

ABSTRACT: 2,3-Dihydrothieno[3,4-*b*][1,4]dioxine-2-carboxylic acid (EDOTacid) is a comonomer for polymers synthesized from 3,4-ethylenedioxythiophene (EDOT) or EDOT derivatives designed to introduce controlled amounts of hydrophilicity into the resulting copolymers. EDOTacid forms a crystalline solid at room temperature; however, its solid-state packing and physical properties were unknown, limiting its ability to be used in various applications. For this purpose, single crystals of EDOTacid grown by various solution and sublimation techniques were characterized by X-ray diffraction, electron microscopy, electron diffraction, thermogravimetric analysis, and polarized optical microscopy. The compound forms orthorhombic crystals with space group *Pbca* (a = 1.014 nm, b = 0.699 nm, c = 2.139 nm, Z = 8, density = 1.63 g/cm^3) per single crystal X-ray diffraction with d-spacings confirmed by powder X-ray diffraction and electron diffraction. The molecules are arranged into hydrogen-bonded dimers, with each member of the pair having opposite handedness. Under a 200 kV electron beam, the EDOTacid crystals showed a critical damage resistance of 15 mC/cm^2, consistent with their observed thermal stability (~146 °C). Scanning electron micrographs of single crystals grown by solvent-evaporation showed a platelet-like morphology with predominant cracks parallel to the b-axis.

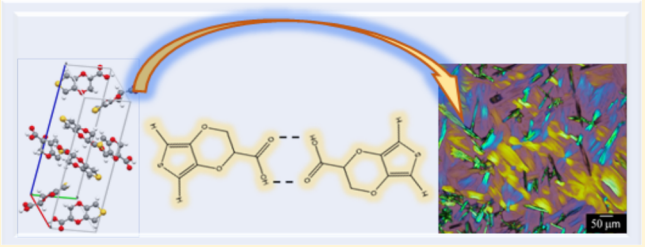

INTRODUCTION

Conjugated polymers have been investigated for a variety of applications including electrochromic displays,[1] photovoltaics,[2] and chemical sensors.[3] They have been of recent interest for interfacing biomedical devices with living tissue because of their ability to conduct charge both electronically and ionically.[4,5] Poly(3,4-ethylenedioxythiophene) (PEDOT) has received particular scientific and commercial attention because of its low oxidation potential, high chemical and thermal stability, and high conductivity.[6,7]

The lack of hydrophilic side groups makes it difficult for the relatively hydrophobic PEDOT to interact with living tissues. 2,3-Dihydrothieno[3,4-*b*][1,4]dioxine-2-carboxylic acid (EDOTacid) (Figure 1) is a comonomer for 3,4-ethylenedioxythiophene (EDOT) designed to introduce controlled amounts of hydrophilicity into the resulting copolymers.[8] Electropolymerized PEDOT−PEDOTacid copolymer films can be coupled with peptides resulting in films with increased bioactivity.[8] These copolymers have a more pleated, open surface texture and higher surface energies than the PEDOT homopolymer.[9] The EDOTacid monomer also has been shown to serve as an adhesion promoter for electropolymerized films of PEDOT.[10] Studies aimed at taking advantage of the carboxylic substitutions in conjugated polymers to increase biological activity and thereby optimize performances of devices like biosensors have also been published.[11−13]

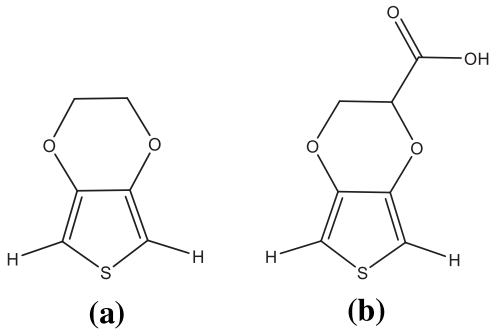

Figure 1. (a) Chemical structures of 3,4-ethylenedioxythiophene (EDOT) and (b) carboxylic acid-functionalized 3,4-ethylenedioxythiophene (EDOTacid)

Although the EDOT monomer (Figure 1a) is a liquid at room temperature, EDOTacid is a crystalline solid. Crystalline organic, small molecules such as pentacene have been used to fabricate thin-film transistors with relatively high mobilities.[14]

Received: May 8, 2019
Revised: September 6, 2019
Published: September 18, 2019

DOI: 10.1021/acs.cgd.9b00613
Cryst. Growth Des. 2019, 19, 6184−6191

EDOT oligomers have also been synthesized and used to study the influence of molecular weight on electronic structure and optical properties.[15] In this study, we show that EDOTacid single crystals have a preferred orientation when deposited onto flat substrates. This can be utilized for other applications like forming textured conducting films for improving the order in homopolymer PEDOT coatings. Thus, this paper focuses on studying properties like crystal structure, shape, electron stability, and thermal stability of EDOTacid crystals to understand their fundamental properties and interactions, giving us insights into improving order in PEDOT polymers and copolymers.

We anticipated that since EDOTacid is reasonably similar to benzoic acid, it might also form hydrogen-bonded dimers in the solid-state. However, since EDOTacid also has a chiral center at the carbon where the carboxylic acid is attached, there will necessarily be enantiomers with opposite left and right handedness present in the as-synthesized racemic mixture. The manner of packing of these enantiomers in the solid-state was not known. The purpose of this paper is to understand the structure−property relationships of EDOT-acid molecular crystals using a variety of characterization techniques including optical and electron microscopy, thermal analysis, and X-ray diffraction. Since crystallinity in P(EDOT-*co*-EDOTacid) copolymers has not yet been thoroughly investigated, this work will also provide some of the necessary groundwork for this purpose. Considering that this would require careful tuning of the pH or using a mixture of solvents to control the precipitation rate of the resulting copolymers to crystallize them, this will be part of a future study.

Transmission electron microscopy (TEM) and electron diffraction (ED) have been widely used for the determination of crystal structures and morphology.[16,17] While X-rays do not cause much damage to the crystallinity in organic materials, the high energy electrons of the TEM cause significant damage.[18,19] This makes it a far more challenging task to image organic materials using TEM. The damage caused by the electron beam can be quantified by estimating the critical electron doses using techniques like ED and electron energy loss spectroscopy (EELS).[20,21] These estimates can then be used to optimize the electron dose used for imaging beam sensitive crystals.

Here, we have used X-ray diffraction, TEM, ED, SEM, polarized optical microscopy, thermal analysis, and molecular simulations to investigate the crystal structure and morphology of EDOTacid and study its interactions with the electron beam.

EXPERIMENTAL SECTION

Materials Used. EDOTacid powder was purchased from Tractus-chemistry and Shanghai Seebio Biotech, LLC and used as received. Dichloromethane (DCM) and acetone were purchased from Thermo Fisher Scientific.

Single Crystal Growth. For performing unit cell structure determinations, relatively large single crystals of EDOTacid (from 10s to 100s of microns in size) were grown by controlled evaporation of a dichloromethane (DCM) solution over a period of about 3 weeks.

Single-Crystal X-ray Diffraction. A crystal of 428 × 110 × 32 μm^3 was obtained by slow evaporation of a dilute (0.0035 wt %) solution of EDOTacid in DCM. Crystals were mounted using viscous oil onto a plastic mesh and cooled to the data collection temperature. Data were collected on a Bruker-AXS APEX II DUO CCD diffractometer with Cu−Kα radiation (λ = 1.54178 Å) focused with Goebel mirrors. Unit cell parameters were obtained from 36 data frames, 0.5° ω, from three different sections of the Ewald sphere (Apex 3).[22] The data were treated with multiscan absorption corrections. The structure was solved using intrinsic phasing methods and refined with full-matrix, least-squares procedures on F^2.[23,24] Non-hydrogen atoms were refined with anisotropic displacement parameters. The carboxylic H atom was located from the electron density difference map and was allowed to refine freely. All other H atoms were treated as idealized contributions with geometrically calculated positions and with U_{iso} equal to 1.2 U_{eq} of the attached atom. Atomic scattering factors are contained in the SHELXTL program library.[24] The structure has been deposited at the Cambridge Structural Database under CCDC 1895659.

Structure and Morphology Characterizations. Transmission electron micrographs and electron diffraction patterns were obtained using a ThermoFisher Talos F200C Scanning Transmission Electron Microscope (STEM) at 200 kV.

Polarized optical micrographs were acquired with a Nikon-Eclipse L200 using a full-wave red filter.

Scanning electron microscopy was performed using a Zeiss Auriga 60 Focused Ion Beam-Scanning Electron Microscope (FIB-SEM) operating at 3 kV.

Powder X-ray diffraction was performed on Bruker D8 diffractometer in a symmetric $\theta/2\theta$ reflection geometry using monochromated Cu−Kα radiation (λ = 1.54 Å) with 2θ ranging from 5° to 70°.

Atomic force microscopy with infrared spectroscopy (AFM-IR) was performed on a Bruker Nano-IR2 (Figure S4).

Physical Properties. Infrared experiments were conducted using a Thermo Nicolet 670 Nexus FT-IR spectrometer with a DTGS detector operating in attenuated total reflection (ATR) mode using a Specac Golden Gate ATR accessory. The spectra were obtained by averaging 128 scans from 600 to 4000 cm^{-1} (Figure S2).

Thermogravimetric analysis was performed on TA Discovery TGA (Figure S3).

Molecular Simulations. Crystal Maker 10 software was used for performing diffraction pattern simulations.[25] Mercury 4.0.0 was used for performing crystal visualization and Bravais Freidel Donner Harkey (BFDH) calculations.[26]

RESULTS AND DISCUSSION

EDOTacid can be readily crystallized by sublimation, solution casting, or slow growth from a polar solvent. Controlled diffusion of a nonpolar solvent into a polar solvent can be used to induce slow precipitation since the molecule is more soluble in polar solvents as compared to nonpolar solvents. EDOTacid is expected to be more soluble in water at high pH due to the presence of the carboxylic acid functional group in the molecule. Highly birefringent single crystals of EDOTacid were readily observed by solution casting from solvents such as acetone, as seen in the polarized optical micrographs in Figure 2a and b. Images obtained with a polarized light and a full wave red filter indicated that the higher refractive index direction was parallel to the long axes of the needle shaped crystals. Slowly, solution-grown single crystals could be formed with overall dimensions of several hundred microns. Long needle crystals were also readily formed by sublimation.

The unit cell of EDOTacid single crystals obtained by slow evaporation of the solvent was estimated from the single crystal X-ray diffraction as follows (Table 1).

The systematic absences in the diffraction data were uniquely consistent with *Pbca* symmetry (space group No. 61). It was also found that the compound was arranged into H-bonded pairs around an inversion center. The atomic positions of EDOTacid molecules are shown in Figure 3 in the [100], [010], and [001] viewing directions. There are eight molecules of EDOTacid per unit cell, resulting in an estimated density of

DOI: 10.1021/acs.cgd.9b00613
Cryst. Growth Des. 2019, 19, 6184−6191

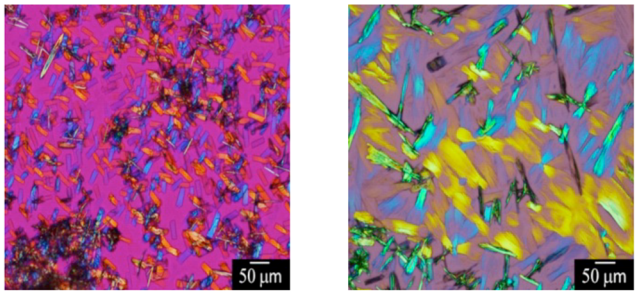

(a) (b)

Figure 2. (a, b) Polarized optical micrographs of solution-cast EDOT acid single crystals obtained with a full-wave red filter. The blue crystals have the higher refractive index direction running from the lower left to upper right, whereas the yellow crystals are oriented with the higher refractive index direction from lower right to upper left. This means the higher refractive index is parallel to the long axes of these needle shaped crystals.

Table 1. Unit Cell Parameters of 2,3-Dihydrothieno[3,4-*b*][1,4]dioxine-2-carboxylic Acid

molecular formula	$C_7H_6O_4S$
molecular weight	186.18 g/mol
space group	*Pbca*
lattice system	orthorhombic
a	1.014 nm
b	0.699 nm
c	2.139 nm
density	1.63 g/cm^3
temperature	200(2) K
Z	8
μ	3.596/mm
R_1 [$I > 2\sigma$]	0.0782
wR_2	0.1873

1.63 g/cm^3. This value is slightly higher than the density of unsubstituted EDOT (1.42 g/cm^3), which is a liquid at room temperature. EDOTacid molecules pack via the formation of hydrogen bonded dimers between the carboxylic acid groups in a manner similar to that seen in benzoic acid (BA) molecules.[27,28] BA packs in a monoclinic unit-cell ($P2_1/c$) where the hydrogen bonded dimers are arranged in a herringbone fashion.[27−29] The herringbone packing can be seen in both EDOTacid and BA crystals, corresponding to the [0$\bar{1}$2] and [10$\bar{4}$] directions, respectively.[27] While the atoms in the BA dimer are all essentially in the same plane, for EDOTacid, some of the atoms lie out of the plane of the thiophene ring. The crystal structure has the EDOTacid molecules paired into dimers, with each pair consisting of one left-handed and one right-handed enantiomer. These enantiomers are paired via hydrogen bonding, which is evident when viewed along the [010] direction (Figure 3b). The packing of the enantiomers alternates along both the *a* and *c* directions with the dimer axis oriented at an angle, which is smallest with respect to the *b* direction. This results in highly anisotropic shapes and mechanical properties, as is observed from the characteristic cracking in the single crystals (Figure 8). The herringbone-like packing motif seen here is quite common in other small molecules such as pentacene and benzoic acid.[30−32] However, what is somewhat different here is that the herringbone crystal packing simultaneously propagates in two different lateral directions, leading to an overall orthorhombic, rather than monoclinic crystal symmetry. BA molecules also form platelet-like crystals that have been observed experimentally and calculated computationally.[31,33]

The positions and relative intensities of the peaks as well as absences due to the symmetry in the simulated pattern (CrystalMaker 10) were fully consistent with the experimental powder pattern (Figure 4a). Thin films formed by solution casting on flat substrates were observed to be highly crystallographically textured by X-ray diffraction measurements. The X-ray pattern of such a textured film taken in a symmetric reflection ($\theta/2\theta$) geometry is shown in Figure 4c, which shows predominant peaks from the (002), (004), and (006) planes, indicating that these are preferentially aligned parallel to the substrate.

Low-dose TEM and ED have been extensively used recently for structure determination of organic small molecules, biological molecules, and proteins.[34−37] Electron microscopy

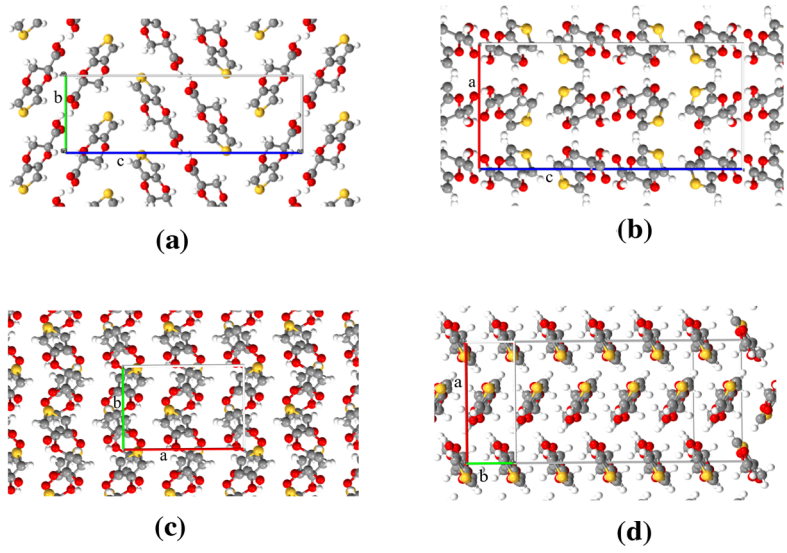

(a) (b) (c) (d)

Figure 3. (a−c) Projections of EDOTacid unit cell along the [100], [010], and [001]. (d) Projection of the herringbone packing observed in EDOTacid molecules, corresponding to the [0$\bar{1}$2] ((002) slice). Axes labels: red, green, and blue colors correspond to *a*, *b*, and *c* axes, respectively.

DOI: 10.1021/acs.cgd.9b00613
Cryst. Growth Des. 2019, 19, 6184−6191

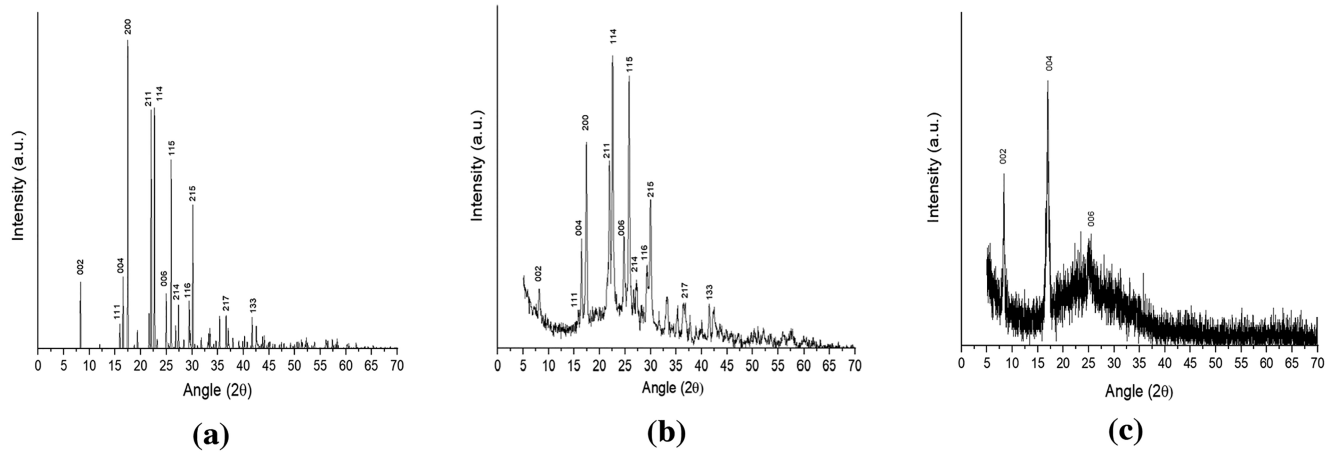

Figure 4. (a) Indexed simulated powder X-ray diffraction pattern of the unit cell (CrystalMaker 10)). (b) X-ray powder diffraction pattern of the EDOTacid powder as received. (c) X-ray pattern of a textured thin-film (taken in a symmetric reflection $\theta/2\theta$ geometry) of EDOTacid deposited from acetone.

makes it possible to examine crystals several orders of magnitude smaller than those needed for traditional crystallographic methods.[37] In addition to using single crystal X-ray diffraction, we used low-dose TEM and ED to study these beam-sensitive slowly grown single crystals from DCM. Some of the crystals were elongated needles with high aspect ratios, while others were more equiaxed. Bright field TEM of both elongated and equiaxed crystals are shown in Figure 5a and b. Contrast variations typical of bend contours were also observed in the crystals. Being sensitive to the electron beam, the bend contours would move continuously through the crystallite before disappearing completely after the sample lost its crystallinity. The ED data were also consistent with the calculated crystal structure. Figure 5c shows the electron diffraction pattern from the single crystal in Figure 5b.

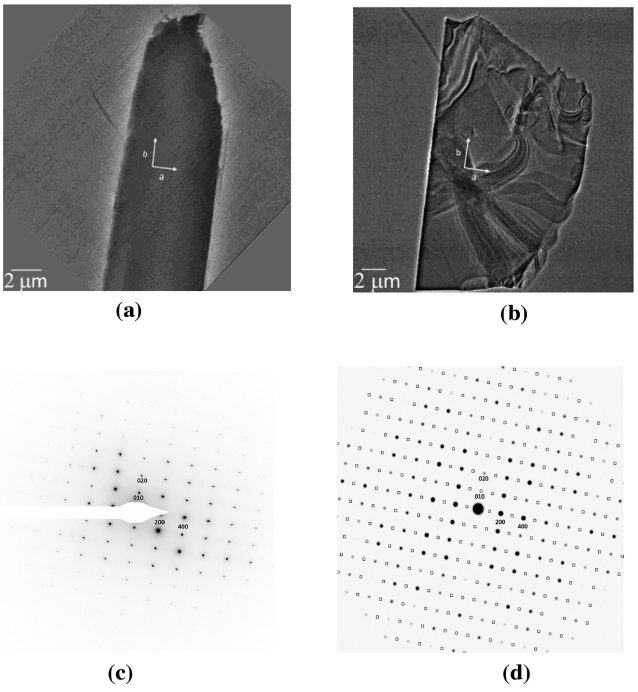

Figure 5. (a) Low dose bright field TEM images of needle-shaped single crystals with high aspect ratio. (b) Low dose bright field TEM image of a single crystal with low aspect ratio. (c) ED pattern from the single crystal in panel b. (d) Simulated ED pattern of the unit cell when viewed along the [001] direction (solid spots are allowed reflections, hollow boxes are forbidden).

Analysis of ED patterns like those shown in Figure 5b showed that the preferred contact plane was (001), corresponding to a preferred zone axis of [001]. The patterns calculated from ED also were consistent with those calculated from unit cell determined from single crystal X-ray diffraction. Figure 5d shows the simulated electron diffraction patterns as viewed from the [001] direction. The absences are due to the glide plane and screw axis symmetries characteristic of the *Pbca* space group. All the absences were observed as expected from the simulations except for the odd (0k0) absences. These on axis absences are violated in the ED presumably due to double diffraction.

The sensitivity of these crystals to the electron beam caused the Bragg reflections to fade as the diffraction patterns were being recorded (Figure 6). The total end-point dose (TEPD) is defined as the electron dose needed for the amorphization of these crystals, and it was estimated to be 15 mC/cm^2. This value is of the same order of the TEPD of polyethylene, which has been reported to be around 3−4 mC/cm^2 at 120 kV.[35] This TEPD value is also in agreement with the thermal stability of EDOTacid (~146 °C, SI, Figure S5). The correlation between the thermal stability of an organic specimen (degradation temperature or melting point) and its electron-beam stability was investigated by Kumar and Adams in 1990.[38] Since the beam-induced damage is attributed to selective bond breakage and their subsequent inability to recombine, Kumar and Adams had an intuitive argument that a specimen with higher thermal stability will require more energy for damage. Additionally, at lower specimen temperatures, more energy (electron dose) is required for damaging the specimen.[21] This can then be related to Kumar and Adams' argument that at lower temperatures, owing to reduced molecular mobility, the probability of recombination of a broken bond is higher.

Figure 7 shows the evolution of the intensity profiles of the (200) and the (220) reflections as a function of electron dose. There were a couple of consistent observations during these experiments. The higher order Bragg reflections faded first followed by the lower order reflections, indicating that higher

DOI: 10.1021/acs.cgd.9b00613
Cryst. Growth Des. 2019, 19, 6184−6191

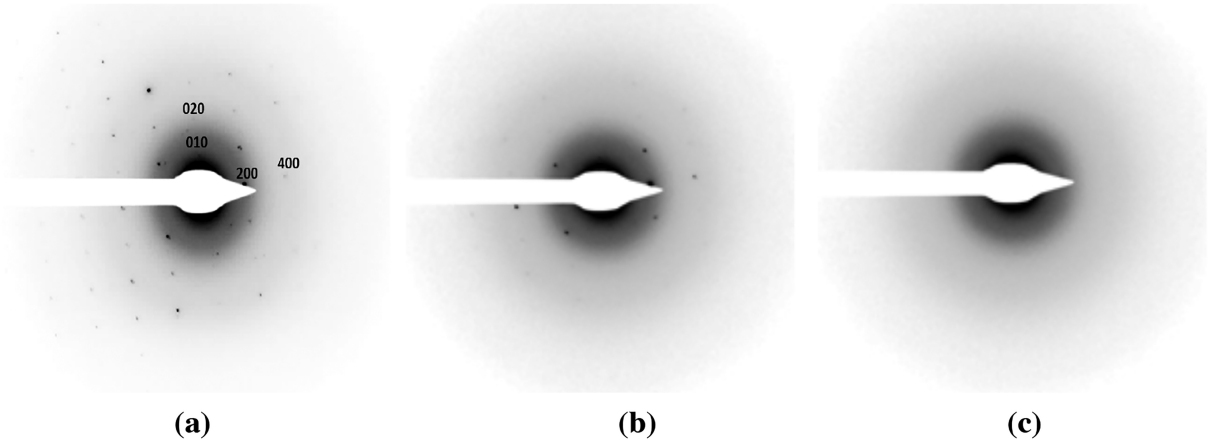

Figure 6. (a–c) Electron diffraction patterns from a single crystal of EDOTacid at electron doses of 0 mC/cm^2, 9 mC/cm^2, and 15 mC/cm^2.

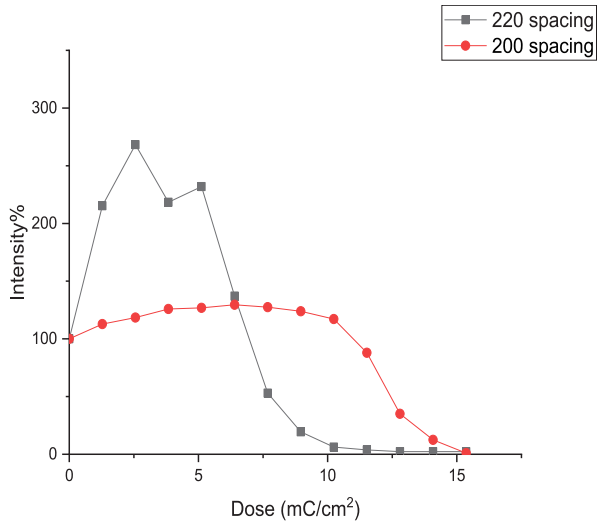

Figure 7. Intensity profiles of diffraction spots of (200) and (220) reflections with increasing electron doses.

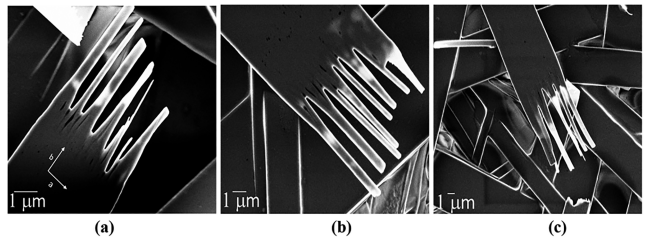

Figure 8. (a–c) Images of the single crystals of EDOTacid as recorded from the scanning electron microscope (Auriga 60 CrossBeam FIB/SEM). The *a* and *b* directions of a single crystal are shown in panel a.

amounts of electron doses are required for the amorphization of the lower order (larger *d*-spacing) reflections. Meaning, short-range order is destroyed, while long-range order still exists. This intermediate state with the long-range order can be compared to a block copolymer consisting of ordered blocks. This state however is not indestructible, and the crystals amorphize after prolonged exposure. Second, we found evidence for a modest increase in intensity and increase in peak width (decrease in effective crystallite size) at intermediate doses. This decrease in effective crystallite size may be due to the bigger crystallites breaking up into smaller ones under continued flux. Similar intermediate states during electron beam irradiation have been seen in other organic and materials like 2,6-bis-octyl-pentathienoacene (C8) and copolymers of poly(vinylidene fluoride).[39,40]

Since the dimer axis is aligned closest to the b direction or the [010] direction, we theorize that it is easier for the EDOTacid single crystals to cleave in the perpendicular directions, thereby causing cracks along directions almost parallel to the *b* direction. This is what we observed experimentally using SEM (Figure 8), which showed roughly rectangular, flat platelets with pronounced cracking parallel to their long axes near the platelet ends. The size and shape of these single crystals varied somewhat with the solvent and the processing conditions. From ED, we know that the EDOTacid crystals go down with their (001) planes preferentially parallel to the substrate (or equivalently, with the [001] direction perpendicular to the substrate) and that the growth rate is highest along the *b* direction [010]. These cracks reveal the local anisotropy of physical properties that results from this molecular arrangement (Figure 3).

Single crystals of EDOTacid were also grown by sublimation. Crystals grown in this manner were faceted and needle shaped and usually larger in all dimensions as compared to the flat, platelet-like morphology that we observe in single crystals from solution. One such crystal is shown in the scanning electron micrograph in Figure 9a. The needle-shaped crystals have thin layers/steps stacked on top of each other in AFM micrographs (Figure S4) with faceting observed primarily on the {002}, {200}, and {220} type surfaces, and occasionally on {111} as well. We compared these observations with the simulated shapes predicted by the Bravais-Friedel-Donnay-Harker (BFDH) method using Mercury 4.0.0 software. The BFDH method uses the symmetry and shape of the unit cell to estimate crystal growth faces and their growth rates but does not account for details in local molecular packing and intermolecular energetics. The overall shape and platelet motif of the EDOTacid crystals were reproduced well (Figure 9b). However, the BFDH method also predicted the existence of some of the faces of {102} type instead of {200} type.

DOI: 10.1021/acs.cgd.9b00613
Cryst. Growth Des. 2019, 19, 6184–6191

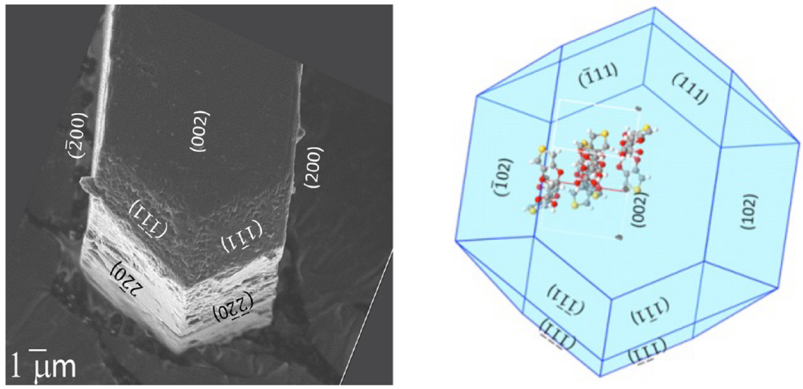

(a) (b)

Figure 9. (a) SEM image of a crystal formed by sublimation of the EDOTacid powder. (b) Simulated shape of the EDOTacid single crystal using BFDH calculations (Mercury 4.0.0).

CONCLUSIONS

We have examined the physical properties and provided a detailed structural characterization of the solid-state packing of EDOTacid. This monomer has already shown the ability to introduce hydrophilicity and bioactivity in P(EDOT-*co*-EDOTacid) copolymers.[8,9] This study additionally shows that the carboxylic acid groups can potentially be used to improve the crystallinity of these conjugated polymers. However, this would require careful control of the pH or use of a combination of solvents to control the precipitation rate and thereby crystallize the polymer chains and will be part of a future study.

We determined the crystal structure based on the data from single crystal X-ray diffraction and corroborating information from TEM, ED, and powder X-ray diffraction. In crystals of EDOTacid, the monomers arranged into hydrogen-bonded dimers, with the two molecules in each dimer having opposite handedness. The dimers are tilted by ∼60 degrees with respect to the *c*-axis. The dimers are oriented closest to the *b* direction, resulting in anisotropic physical properties in the single crystals. This was observed in crystals formed by precipitation from solution, which were predominantly flat platelets, with cracks parallel to the *b* direction. As compared to the solution-grown single crystals, crystals grown by sublimation were much more elongated and needle-shaped with faceting observed primarily on the {002}, {200}, {220}, and {111} type planes.

Our research group has been investigating the nucleation and growth of electrodeposition of polythiophenes, particularly PEDOT and its derivatives, to optimize properties of the final polymer.[41] For us to be able to perform similar reactions with EDOTacid in TEM and understand its growth mechanisms, we need to have an estimate of its electron beam stability. Consequently, we obtained the electron-beam stability to be ∼15 mC/cm^2, which is consistent with its thermal stability of ∼146 °C. In like manner, we hope our physical characterization of EDOTacid presented promotes better utility in current PEDOT applications and spurs further new applications.

ASSOCIATED CONTENT

Supporting Information

The Supporting Information is available free of charge on the ACS Publications website at DOI: 10.1021/acs.cgd.9b00613.

Solubility calculations for EDOTacid as function of pH, Fourier transform infrared spectrum of EDOTacid, thermogravimetric analysis, atomic force micrograph−infrared spectrum from crystals obtained by sublimation, low-dose high resolution image of EDOT acid thin-film, $1/d^2$ values for experimentally obtained powder diffraction data (PDF)

Accession Codes

CCDC 1895659 contains the supplementary crystallographic data for this paper. These data can be obtained free of charge via www.ccdc.cam.ac.uk/data_request/cif, or by e-mailing data_request@ccdc.cam.ac.uk, or by contacting The Cambridge Crystallographic Data Centre, 12 Union Road, Cambridge CB2 1EZ, UK; fax: +44 1223 336033.

AUTHOR INFORMATION

Corresponding Author

*E-mail: milty@udel.edu.

ORCID

David C. Martin: 0000-0003-1195-3838

Author Contributions

The experimental work, with the exception of the single crystal X-ray diffraction, was done by V.S. The X-ray single crystal data acquisition and analysis were done by C.A.R. and G.P.A.Y. V.S. wrote the original draft of the manuscript, with considerable revisions and assistance in the data analysis and presentation by D.C.M. All authors have reviewed and given approval to the manuscript.

Notes

The authors declare no competing financial interest.

ACKNOWLEDGMENTS

The authors would like to thank Gerald Poirier, Dr. Jing Qu, Dr. Roddel Remy, Prof. Bruce Chase, and Changhao Liu for their assistance with experiments and their valuable input. The authors also gratefully acknowledge access to and support from the Keck Centre for Advanced Microscopy and Microanalysis, and the Advanced Materials Characterization laboratory at the University of Delaware. This work was supported by the National Science Foundation (DMR-1808048).

DOI: 10.1021/acs.cgd.9b00613
Cryst. Growth Des. 2019, 19, 6184−6191

REFERENCES

(1) Kawahara, J.; Ersman, P. A.; Engquist, I.; Berggren, M. Improving the Color Switch Contrast in PEDOT:PSS-Based Electrochromic Displays. *Org. Electron.* **2012**, *13* (3), 469−74.

(2) Ikeda, N.; Koganezawa, T.; Kajiya, D.; Saitow, K. Performance of Si/PEDOT:PSS Hybrid Solar Cell Controlled by PEDOT:PSS Film Nanostructure. *J. Phys. Chem. C* **2016**, *120* (34), 19043−48.

(3) Zhu, Z.-T.; Mabeck, J. T.; Zhu, C.; Cady, N. C.; Batt, C. A.; Malliaras, G. G. A Simple Poly(3,4-Ethylene Dioxythiophene)/Poly(Styrene Sulfonic Acid) Transistor for Glucose Sensing at Neutral PH. *Chem. Commun.* **2004**, *0* (13), 1556−57.

(4) Martin, D. C. Molecular Design, Synthesis, and Characterization of Conjugated Polymers for Interfacing Electronic Biomedical Devices with Living Tissue. *MRS Commun.* **2015**, *5* (02), 131−53.

(5) Rivnay, J.; Inal, S.; Collins, B. A.; Sessolo, M.; Stavrinidou, E.; Strakosas, X.; Tassone, C.; Delongchamp, D. M.; Malliaras, G. G. Structural Control of Mixed Ionic and Electronic Transport in Conducting Polymers. *Nat. Commun.* **2016**, *7*, 11287.

(6) Groenendaal, B. L.; Jonas, F.; Freitag, D.; Pielartzik, H.; Reynolds, J. R Poly(3,4-ethylenedioxythiophene and Its Derivatives : Past, Present, and Future. *Adv. Mater.* **2000**, *12* (7), 481−494.

(7) Crispin, X.; Jakobsson, F. L. E.; Crispin, A.; Grim, P. C. M.; Andersson, P.; Volodin, A.; van Haesendonck, C.; Van der Auweraer, M.; Salaneck, W. R.; Berggren, M. The Origin of the High Conductivity of Poly(3,4-Ethylenedioxythiophene)−Poly-(Styrenesulfonate) (PEDOT−PSS) Plastic Electrodes. *Chem. Mater.* **2006**, *18* (18), 4354−60.

(8) Povlich, L. K.; Cho, J. C.; Leach, M. K.; Corey, J. M.; Kim, J.; Martin, D. C. Synthesis, Copolymerization and Peptide-Modification of Carboxylic Acid-Functionalized 3,4-Ethylenedioxythiophene (EDOTacid) for Neural Electrode Interfaces. *Biochim. Biophys. Acta, Gen. Subj.* **2013**, *1830* (9), 4288−4293.

(9) Bhagwat, N.; Kiick, K. L.; Martin, D. C. Electrochemical Deposition and Characterization of Carboxylic Acid Functionalized PEDOT Copolymers. *J. Mater. Res.* **2014**, *29* (23), 2835−44.

(10) Wei, B.; Liu, J.; Ouyang, L.; Kuo, C.-C.; Martin, D. C. Significant Enhancement of PEDOT Thin Film Adhesion to Inorganic Solid Substrates with EDOT-Acid. *ACS Appl. Mater. Interfaces* **2015**, *7* (28), 15388−15394.

(11) Mouffouk, F.; Higgins, S. J. Oligonucleotide−Functionalised Poly(3,4-Ethylenedioxythiophene)-Coated Microelectrodes Which Show Selective Electrochemical Response to Hybridisation. *Electrochem. Commun.* **2006**, *8* (2), 317−22.

(12) Lee, J.-W.; Serna, F.; Nickels, J.; Schmidt, C. E. Carboxylic Acid-Functionalized Conductive Polypyrrole as a Bioactive Platform for Cell Adhesion. *Biomacromolecules* **2006**, *7* (6), 1692−95.

(13) Kwon, O. S.; Park, C. S.; Park, S. J.; Noh, S.; Kim, S.; Kong, H. J.; Bae, J.; Lee, C.-S.; Yoon, H. Carboxylic Acid-Functionalized Conducting-Polymer Nanotubes as Highly Sensitive Nerve-Agent Chemiresistors. *Sci. Rep.* **2016**, *6*, 33724.

(14) Newman, C. R.; Chesterfield, R. J.; Panzer, M. J.; Daniel Frisbie, C. High Mobility Top-Gated Pentacene Thin-Film Transistors. *J. Appl. Phys.* **2005**, *98* (8), 084506.

(15) Apperloo, J. J.; Groenendaal, L.; Verheyen, H.; Jayakannan, M.; Janssen, R. A. J.; Dkhissi, A.; Beljonne, D.; Lazzaroni, R.; Brédas, J.-L. Optical and Redox Properties of a Series of 3,4-Ethylenedioxythiophene Oligomers. *Chem - Eur J* **2002**, *8* (10), 2384−96.

(16) Shaw, C. M.; Zhang, X.; San Miguel, L.; Matzger, A. J.; Martin, D. C. Synthesis and Structure of α-Substituted Pentathienoacenes. *J. Mater. Chem. C* **2013**, *1* (23), 3686.

(17) Chen, J.; Martin, D. C.; Anthony, J. E. Morphology and Molecular Orientation of Thin-Film Bis(Triisopropylsilylethynyl) Pentacene. *J. Mater. Res.* **2007**, *22* (06), 1701−9.

(18) Libera, M. R.; Egerton, R. F. Advances in the Transmission Electron Microscopy of Polymers. *Polym. Rev.* **2010**, *50* (3), 321−39.

(19) Martin, D. C.; Wu, J.; Shaw, C. M.; King, Z.; Spanninga, S. A.; Richardson-Burns, S.; Hendricks, J.; Yang, J. The Morphology of Poly(3,4-Ethylenedioxythiophene). *Polym. Rev.* **2010**, *50* (3), 340−384.

(20) Guo, C.; Allen, F. I.; Lee, Y.; Le, T. P.; Song, C.; Ciston, J.; Minor, A. M.; Gomez, E. D. Probing Local Electronic Transitions in Organic Semiconductors through Energy-Loss Spectrum Imaging in the Transmission Electron Microscope. *Adv. Funct. Mater.* **2015**, *25* (38), 6071−6076.

(21) Leijten, Z. J. W. A.; Keizer, A. D. A.; de With, G.; Friedrich, H. Quantitative Analysis of Electron Beam Damage in Organic Thin Films. *J. Phys. Chem. C* **2017**, *121* (19), 10552−10561.

(22) *Apex3*; Bruker AXS Inc.: Madison, WI, 2015.

(23) Sheldrick, G. M. SHELXT − Integrated Space-Group and Crystal-Structure Determination. *Acta Crystallographica Section A: Foundations and Advances* **2015**, *71* (1), 3−8.

(24) Sheldrick, G. M. Crystal Structure Refinement with *SHELXL*. *Acta Crystallographica Section C Structural Chemistry* **2015**, *71* (1), 3−8.

(25) Palmer, D. C. *CrystalMaker 10*; CrystalMaker Software Ltd: Begbroke, Oxfordshire, England, 2014.

(26) Macrae, C. F.; Edgington, P. R.; McCabe, P.; Pidcock, E.; Shields, G. P.; Taylor, R.; Towler, M.; van de Streek, J. Mercury: Visualization and Analysis of Crystal Structures. *J. Appl. Crystallogr.* **2006**, *39* (3), 453−57.

(27) Sim, G. A.; Robertson, J. M.; Goodwin, T. H. The Crystal and Molecular Structure of Benzoic Acid. *Acta Crystallogr.* **1955**, *8* (3), 157−64.

(28) Feld, R.; Lehmann, M. S.; Muir, K. W.; Speakman, J. C. The Crystal Structure of Benzoic Acid: A Redetermination with X-Rays at Room Temperature. *Z. Kristallogr. - Cryst. Mater.* **1981**, *157* (3/4), 215−31.

(29) Dubey, R.; Pavan, M. S.; Desiraju, G. R. Structural Landscape of Benzoic Acid: Using Experimental Crystal Structures of Fluorobenzoic Acids as a Probe. *Chem. Commun.* **2012**, *48* (72), 9020−22.

(30) Tang, W.; Zhang, M.; Mo, H.; Gong, J.; Wang, J.; Li, T. Higher-Order Self-Assembly of Benzoic Acid in Solution. *Cryst. Growth Des.* **2017**, *17* (10), 5049−53.

(31) Holmbäck, X.; Rasmuson, Å. C. Size and Morphology of Benzoic Acid Crystals Produced by Drowning-out Crystallisation. *J. Cryst. Growth* **1999**, *198−199*, 780−88.

(32) Drummy, L. F.; Miska, P. K.; Alberts, D.; Lee, N.; Martin, D. C. Imaging of Crystal Morphology and Molecular Simulations of Surface Energies in Pentacene Thin Films. *J. Phys. Chem. B* **2006**, *110* (12), 6066−71.

(33) Liang, Z.; Zhang, M.; Wu, F.; Chen, J.-F.; Xue, C.; Zhao, H. Supersaturation Controlled Morphology and Aspect Ratio Changes of Benzoic Acid Crystals. *Comput. Chem. Eng.* **2017**, *99*, 296−303.

(34) Hattne, J.; Shi, D.; Glynn, C.; Zee, C.-T.; Gallagher-Jones, M.; Martynowycz, M. W.; Rodriguez, J. A.; Gonen, T. Analysis of Global and Site-Specific Radiation Damage in Cryo-EM. *Structure* **2018**, *26* (5), 759−766.e4.

(35) Nannenga, B. L.; Gonen, T. Protein Structure Determination by MicroED. *Curr. Opin. Struct. Biol.* **2014**, *27*, 24−31.

(36) Nannenga, B. L.; Bu, G.; Shi, D. The Evolution and the Advantages of MicroED. *Frontiers in Molecular Biosciences* **2018**, *5*, 114 DOI: 10.3389/fmolb.2018.00114.

(37) Liu, S.; Hattne, J.; Reyes, F. E.; Sanchez-Martinez, S.; Jason de la Cruz, M.; Shi, D.; Gonen, T. Atomic Resolution Structure Determination by the Cryo-EM Method MicroED. *Protein Sci.* **2017**, *26* (1), 8−15.

(38) Kumar, S.; Adams, W.W. Electron Beam Damage in High Temperature Polymers. *Polymer* **1990**, *31* (1), 15−19.

(39) Wu, J.; Shaw, C. M.; Martin, D. C. 2.19 - Electron Microscopy of Organic Materials: An Overview and Review of Recent Developments. *Polymer Science: A Comprehensive Reference* **2012**, 509−25.

(40) Lovinger, A. J. Polymorphic Transformations in Ferroelectric Copolymers of Vinylidene Fluoride Induced by Electron Irradiation. *Macromolecules* **1985**, *18* (5), 910−18.

(41) Liu, J.; Wei, B.; Sloppy, J. D.; Ouyang, L.; Ni, C.; Martin, D. C. Direct Imaging of the Electrochemical Deposition of Poly(3,4-

DOI: 10.1021/acs.cgd.9b00613
Cryst. Growth Des. 2019, 19, 6184−6191

Ethylenedioxythiophene) by Transmission Electron Microscopy. *ACS Macro Lett.* **2015**, *4* (9), 897−900.

DOI: 10.1021/acs.cgd.9b00613
Cryst. Growth Des. 2019, 19, 6184−6191